Peer-reviewed version available at Polymers 2018, 10, 862; doi:10.3390/polym10080862

Type of the Paper (Article.)

Preparation ofCuONPs@PVDF/non-woven polyester composite membrane: structural influence of nanoparticles addition

Claudio A. Terraza[aφ], Rudy Martin[a], Cesar Saldías[b], MarjorieGonzález[a], Ángel Leiva[bφ], Alain Tundidor-Camba[aφ*]**

[a]Research Laboratory for Organic Polymers (RLOP), Faculty of Chemistry, Pontificia Universidad Católica de Chile, *P.O. Box 306, Post 22*,Santiago, Chile.
[b]Department of Physical Chemistry, Faculty of Chemistry, Pontificia Universidad Católica de Chile, *P.O. Box 306, Post 22*,Santiago, Chile.
[φ]Energy Research Center. Pontificia Universidad Católica de Chile, Chile
*Correspondence: atundido@uc.cl; Tel: +56 223541199
** Correspondence: aleivac@uc.cl; Tel: +56 223544392

Abstract: Membrane distillation techniques appear as one of the most promise alternative to guarantee the availability of potable water in time of scarce of this essential resource. For membrane preparation, polyvinylidene fluoride (PVDF) is preferred due to the easier synthesis procedures with respect to other fluorine based polymers. In this work, copper oxide nanoparticles (CuONPs) at different weight percent (wt.%), embedded in PVDF membranes supported on non-woven polyester fabric (NWPET) were prepared by the phase-inversion method, and characterized by spectroscopy (ATR-FTIR, Raman) and electron microscopy techniques (SEM). The PVDF deposited onto the NWPET was highly composed by its polar -phase (F( )= 53 %) which was determined from the ATR-FTIR spectrum. The F( ) value was kept constant, in the whole range of CuONPs studied (2-10 wt.%) as was determined from the ATR-FTIR spectrum. The absence of signals corresponding to CuONPs in the ATR-FTIR spectra and the appearance of peaks at 297, 360 and 630 cm-1 in the Raman spectra of the membranes suggested that the CuONPs are preferably located in the inner of the membrane but not on its surface. The membrane morphologies were characterized by SEM. From the obtained SEM micrographs, a decrease and increase in the amount of micropores and nanopores, respectively, near to the surface and intercalated in the finger-like layer were observed. As result of the CuONPs addition, the nanopores in the sponge-like layer decrease in size. The values of water contact angle (WCA) measurements showed a trend to decrease from 94° to 80° upon the addition of CuONPs (2-10 wt.%) indicating a diminish in the hydrophobicity degree of the membranes. Apparently, the increase in the amount of nanopores near to the surface decreased the membrane roughness becoming less hydrophobic.

Keywords: Membrane distillation, polyvinylidene fluoride, copper oxide nanoparticles, membrane morphology.

1. Introduction

It is expected that for 2025, the total water shortage will affect 1.8 billion people around the world and the 66% of total populations could be living under water stress conditions. The need to find adequate technologies to supply water and guarantee the livelihood of the human being is a task to accomplish in the short-medium term. Oceans represent the ~97% of the global water reserves and therefore water desalinization techniques have gained the attention to fulfill its demand in a potable form [1]. Accordingly, Membrane Distillation (MD) technique appears as one of the most promising technologies to obtain potable water from seawater [2].

Membrane distillation is a separation process from which vapor molecules of water, driven by a thermal gradient, pass through a porous hydrophobic membrane [3]. This technique displays several advantages compared to other existing ones (thermal desalinization and reverse osmosis), such as a very high rejection of non-volatile solute, lower operating temperature and pressure and the possibility to use low-grade energy sources (e.g., waste heat) as well as the use of renewable energy sources (e.g., solar and geothermal). The reasons mentioned above not only make the MD an economically feasible solution but also emerges as an environmentally friendly alternative for water purification.

Considering the characteristics of the separation process, the membranes for MD should have high permeability, low tendency to fouling, high chemical and thermal stability and a relatively high hydrophobic degree. These features can be achieved by controlling the thickness, porosity, mean pore size, pore size distribution, geometry and composition of the membranes. The hydrophobicity is a crucial parameter and should be high enough to withstand a high liquid entry pressure (LEP). This should allow that only the water vapor enters the pores of the membrane without moistening[1,3].

The most common hydrophobic membranes used for MD are made up of fluoropolymers. From this type of polymers i.e., polytetrafluoroethylene (PTFE) and polyvinylidene fluoride (PVDF) has been widely applied due to their higher mechanical, chemical and heat resistance in comparison with other hydrophobic materials [1]. Although PTFE is the most hydrophobic, it exhibits low solubility in commons solvents, membranes fabricated from this polymer should be obtained by stretching or thermal methods which lead to a relatively low porosity and restricts their processability. Conversely, PVDF is soluble in varied common solvents which would allow the incorporation of several additives, for the purpose of achieving new properties and preparation of hierarchical composite membranes via non-solvent induced phase separation (NIPS) process or via phase inversion techniques [4].

Important issues should be considered for the preparation of MD membranes with industrial applications which are related to the mass flux, heat loss across the membrane, fouling problems and mechanical strength. As inferred, these issues would play a key role in the efficiency of the process. Flat-sheet PVDF membranes supported in non-woven polyester fabric (NWPET) yield hydrophilic/hydrophobic layers wich additionaly to accomplish with the mass flux increases and avoids the heat loss, confers significantly mechanical strength to the membrane. [1,3,5].

The modification of roughness and hydrophobicity of the membrane for increasing the efficiency in separation has also been addressed in the past. A direct way to tune these parameters is by incorporating inorganic nanoparticles into the membrane [4,6]. A widely used simple method to incorporate such type of nanoparticles is by adding into a polymer solution [4,7,8]. Several inorganic nanoparticles such TiO_2, SiO_2, $Mg(OH)_2$, Al_2O_3, ZnO, $CaCO_3$ have been incorporated into PVDF membranes [4,9–12]. In this context, an type of metal nanoparticles that potentially would enable to improve the performance and properties of MD is copper oxide nanoparticles (CuONPs). To the best our knowledge, the use and properties of CuONPs in MD preparation (compared to other types of metal oxide nanoparticles) has been scarcely reported in literature to date. [13–15].

CuONPs embedded into PVDF membranes trend to enlarge the surface pores and thickening the finger-like layer [14,15]. This structural membrane features induced an increase in flux by ~150 % at relatively low working-temperature (27.5 °C). Interestingly, the incorporation of CuONPs did not dramatically affect the membrane selectivity [14]. Recently, Zhao et. al prepared PVDF composite

membranes using copper oxide nanoparticles and graphene oxide as nanofillers[15]. The obtained composite membrane showed a higher permeation since resulted in finger-like macro-voids and thinner interconnected pores when compared to the non-filled membrane.

Although in the literature it is reported the preparation of CuONPs PVDF composite membranes and PVDF membranes supported onto NWPET, none of the encountered reports deal with the combination of both features. Accordingly and based on these previous reports it is probable that the best performance of the here obtained membrane occurs in direct contact or vacuum membrane distillation setups[14,16]

In the present work, we prepared and characterizeda novel CuONPs embedded PVDF composite membrane, as the hydrophobic layer, supported onto non-woven polyester fabric as the hydrophilic layer. Special emphasis is placed on the presence of the CuONPs which would influence the size and morphology of the pores in each sublayer of the membrane. Additionally, acorrelation between the values of water contact angles with the size of the pores distributed along the membrane was detected. The motivation to carry out the study of the preparation and characterization of these hydrophobic/hydrophilic composite membranes arises in order to offer potential alternatives for technological solutions related to the water supply in the future.

2. Materials and Methods

Polydivinylfluoride (PVDF), copper (II) sulfate pentahydrate ($CuSO_4$ x 5 H_2O, 98.0 %) and *N,N*-dimethtylformamide (DMF) were purchased from Sigma-Aldrich (Milwaukee, WI, USA) and were used without further purification. Non-woven polyester fabric (NWPET) was purchased from ImportadoraDilaco S.A. (Santiago, Chile).

Preparation of CuONPs

Copper oxide nanoparticles (CuONPs) were prepared using DMF as reducing and stabilizing agent according to the previous reports in literature[17,18]. Typically, $CuSO_4$ x 5 H_2O (0.2 g) was poured into a two-neck glass flask containing DMF (10 mL). The flask was connected to a reflux system and heated to 120 °C for 5 h under constant stirring. The solution color turned from a light green to yellowish as the copper oxide nanoparticles were formed. This solution served as stock for the preparation of the doped CuONPs/PVDF membranes at different compositions.

Preparation of composite NWPET-PVDF membranes neat and doped with CuONPs

Selection of PVDF concentration for preparing the films

The composite NWPET-PVDF membranes were prepared by the phase inversion method as follows: The casting solutions (1mL) at different PVDF concentrations (25 mg/mL, 50 mg/mL and 200 mg/mL) were stirred for 24 h at room temperature to guarantee a homogeneous polymer solution. The resulting casting solutions were spread onto the NWPET fabric helped by a made-hand alumina template (~1 mm of thickness), in order to minimize the polydispersity in films thickness (Figure 1). The solutions spread on the NWPET surface was left stand for 20 s before they were sinking, for 24 h, in distilled water at 25 °C to promote the precipitation of the PVDF. The prepared composite membranes were left dried in a desiccator with P_2O_5 for further use.

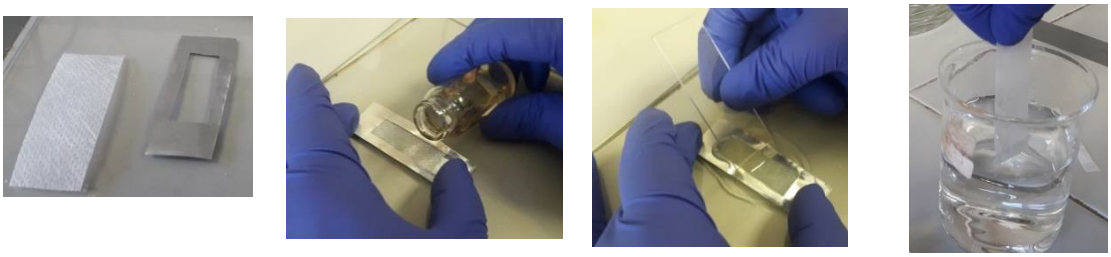

Figure 1. Methodology used for preparing composite membranes.

Preparation of the NWPET-PVDF composite membranes doped with CuONPs

The CuONPs embedded in the membranes were prepared similar to as was mentioned above but previously dissolving the PVDF (200 mg) in DMF solutions of CuONPs (1 mL) prepared from the CuONPs stock solution (the volumes were adjusted to obtain 2, 4, 6, 8 and 10 wt.% CuONPs/PVDF). The previously mixed solutions of PVDF and CuONPs were sonicated during 30 min to guarantee the dispersion of nanoparticles in the whole volume. Then, the solutions were spread over the NWPET surface as was mentioned before.

Membrane morphology studies

The membrane morphology was studied using a Scanning Electron Microscope Zeizz, model EVO MA 10. The cross-section SEM micrographs were acquired by fracturing the membranes using liquid nitrogen to freeze them and a surgical scalpel to cut the NWPET. The membranes were coated with gold, using a Cressington-108 auto Sputter Coater. The measures and process of the obtained SEM micrographs was performed using the free ImageJ (version 1.46J/Fiji) software from the National Institute of Health. USA[19].

ATR-FT-IR and Raman spectroscopy

Infrared spectra were recorded on a Perkin-Elmer Spectrum-Two spectrometer with a UATR unit coupled. The deposited polyester PVDF face was directly positioned over the diamond, pressed until the 30% of the total supported pressure and scanned in the range of 4000 to 500 cm^{-1} with a resolution of 1 cm^{-1}. The β-phase fraction ($F(\beta)$) of the different PVDF covered NWPET was determined from the absorbance of the IR bands at 764 cm^{-1}(A_α)and 840 cm^{-1}(A_β)using the equation 1[20].

$$F(\beta) = \frac{A_\beta}{1.26A_\alpha + A_\beta} \quad (1)$$

Raman Spectra were recorded on a DeltaNu benchtop Raman spectrophotometer with a 785 nm laser. For each sample, ten spectra were recorded for each one with a 5s of integration time.

Contact angle measurements

The contact angle was determined by the technique of the sessile drop using a Dataphysics OCA 20. A syringe, connected to a capillary of Teflon of approximately 2 mm of internal diameter was used to deposit the water drop on the samples. All measurements were done at room temperature. The acquisition of the images was carried out by computational processing of the drop profile on the membranes.

3. Results and Discussion

3.1 Determination of PVDF concentration to prepare the composite membranes

The concentration of PVDF solution to ensure the total covering of the NWPET surface was determined by spreading, onto the fabric, polymer solutions at 25, 50 and 200 mg/mL and recording the SEM micrograph of the obtained surfaces (Figure 2).

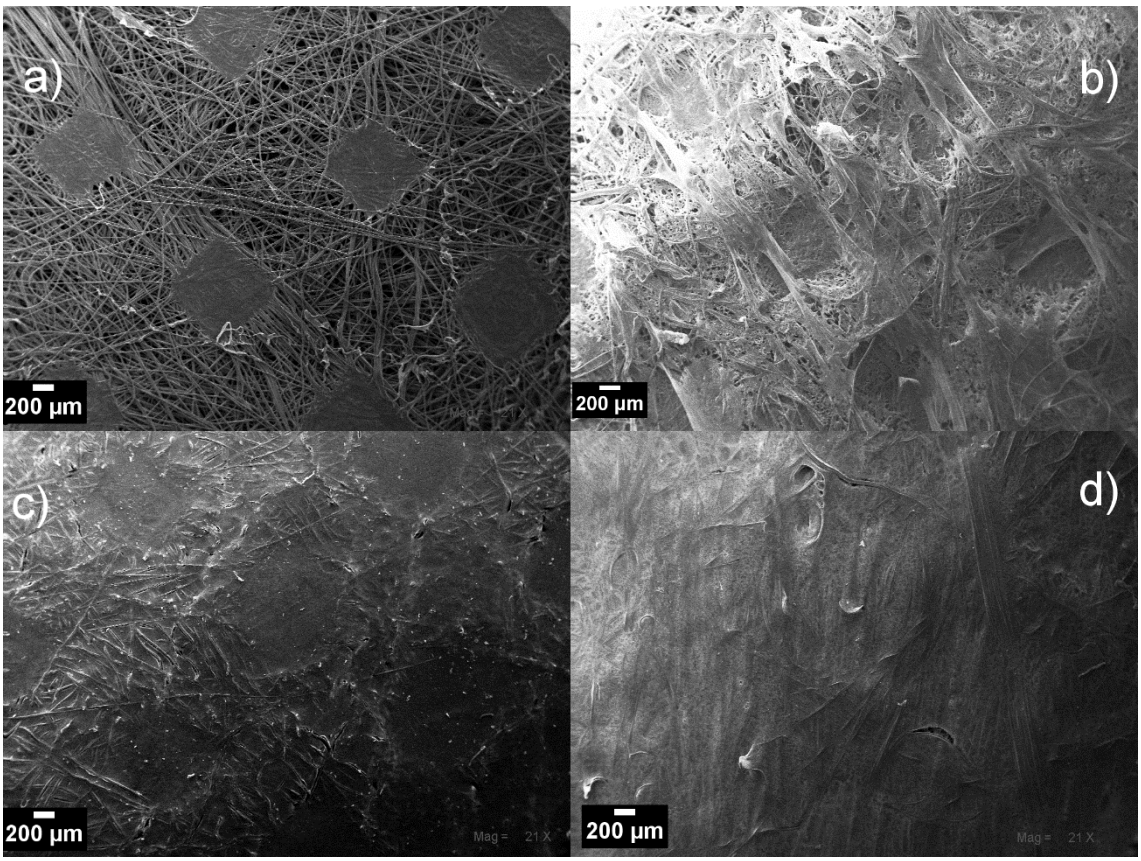

Figure 2. SEM micrograph of a) neat NWPET fiber (a) and covered by depositing the casting solution at b) 25 g/L, c) 50 g/L and d) 200 g/L of PVDF concentration. (Magnification 21x; scale bar 200 µm).

The NWPET fabric is composed of PET fibers randomly aligned and jointed by the pressing of the fabric (squares shapes in Figure 2a). As can be noted, by using the lowest PVDF concentration (Figure 2b) a heterogeneous surface morphology was obtained. At this concentration, the polymer amount is not enough to cover all the surface showing certain domains of the PVDF films intercalated within the NWPET. When the PVDF concentration is incremented to 50 mg/mL, the surface appears totally covered; however the pattern of the pressed fabric and also the fibers contours are observed (Figure 2c). This would indicate that despite the film thickness a homogeneous surface is not observed. At the highest PVDF concentration, the surface is apparently covered (Figure 1d) although some fabric fibers (it is likely that those fibers are far from the pressure zones far from the pressing zones) still emerging at the surface of films as detected by ATR-FTIR spectroscopy. Thereby, we considered that this concentration (200 mg/mL) was adequate to prepare the flat-sheet surfaces as higher concentration the viscosity of the medium increased considerably..

3.2 ATR-FT-IR and Raman CuO@PVDF Characterization

The PDVF covered NWPET prepared in absence and presence of CuONPs were characterized by ATR-FT-IR and Raman spectroscopy (Figure 3). Figure 3a shows the ATR-FT-IR spectra recorded to the neat and covered NWPET with PVDFfilms. The FT_IR spectrum of neat NWPET shows the characteristic peaks of this material at 1713 cm^{-1} (-CO stretching), 1238 cm^{-1} (-C(CO)O- stretching)

Peer-reviewed version available at Polymers 2018, 10, 862; doi:10.3390/polym10080862

and 1092 cm^{-1} (-OCC- stretching). When PVDF solution was spread over NWPET surface, the peaks at 1713 cm^{-1} and 1238 cm^{-1} decrease in intensity while the peak at 1092 is overlapped by a new intense band at 1182 cm^{-1}. This band corresponds to the asymmetric stretch of the -CF_2 while the symmetric component was recorded at 1073 cm^{-1}.

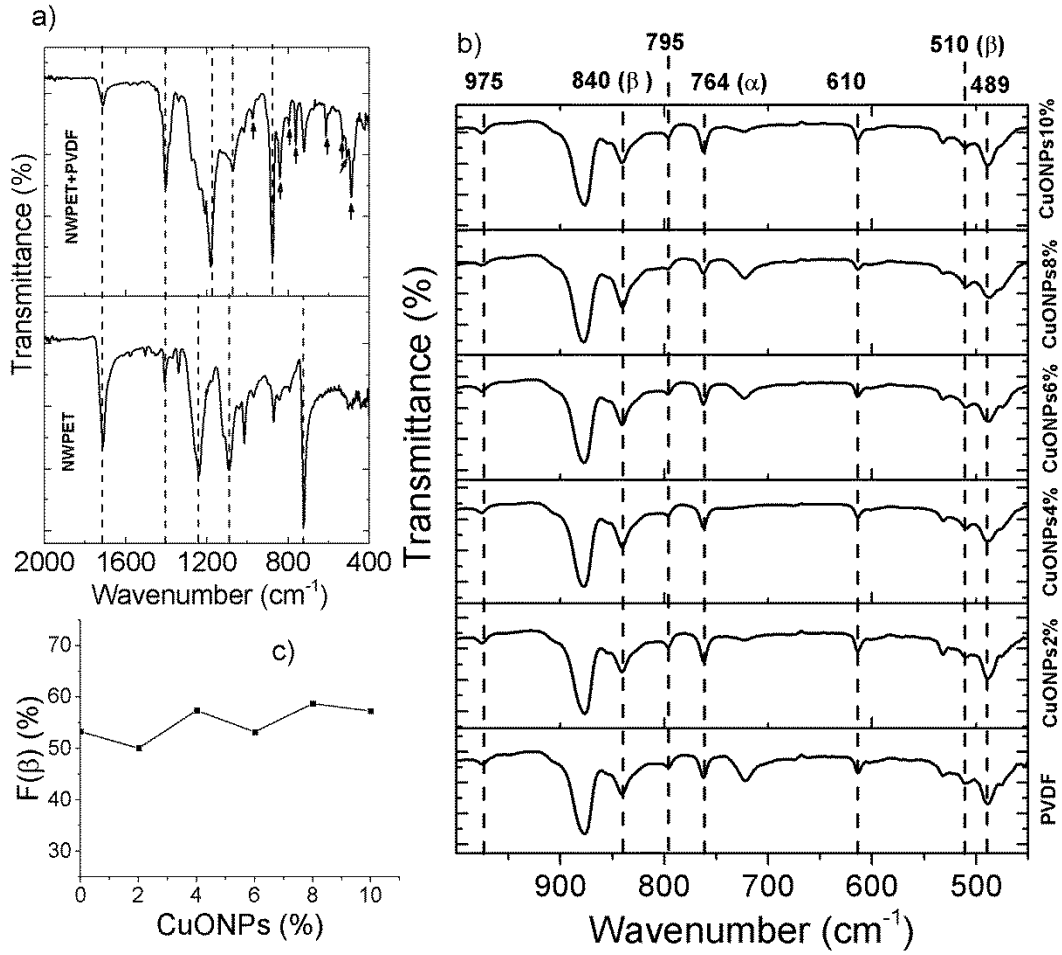

Figure 3. ATR-FTIR spectra of a) neat NWPET and PVDF covered NWPET and b) NWPET-PVDF membranes prepared at different CuONPs/PVDF compositions. c) Dependence of the β-phase fraction with the CuONPs/PVDF composition.

The infrared spectrum of PVDF mainly covers the low wavenumber region (Figure 3b). The -CF_2 wagging (489 cm^{-1}) and bending (610 cm^{-1}), the skeletal bending (764 cm^{-1}), the -CH_2 rocking (795 cm^{-1}) and twisting (975 cm^{-1}) are some of the peaks characteristic of the non-polar α-phase of PVDF (indicated by black arrows, Figure 3a) [13,21,22]. Two peaks, labeled with black arrows in Figure 3a (at 510 cm^{-1} and 840 cm^{-1}corresponding to the -CF_2 stretching -CH_2 rocking, respectively) were also recorded. These peaks would indicate the presence of a β-phase of the PVDF (β-PVDF). The intensity of the peak at 840 cm^{-1} suggests an important contribution of the polar β-PVDF to the polymer structure. Interestingly, in neat PVDF prepared by phase inversion methods, the fraction of the polar β-phase in the polymer structure is very low ($F(\beta)$<35%) [13,22]. The $F(\beta)$ value of the polymer deposited onto the non-woven PET indicates that the 53 % corresponds to the β-phase. These results suggest that the adhesion of the PVDF to NWPET favors the β-phase conformation. Thereby, the observed changes in the intensities of the signals as well as the presence of others additional corresponding to the PVDF, help confirm the presence of the polymer on the NWPET surface.

The infrared spectrum of the PVDF films prepared in presence of CuONPs is shown in Figure 3b). Apparently, the presence of CuONPs did not dramatically affect the intensity and wavenumber

of the signals. (note the signals labeled by dashed lines). To verify the effect of the addition of CuONPs in the crystallinity of the polymer, the fractions of $F(\beta)$ were determined (Figure 3c) for each sample.

It is reported that the addition of metal oxide nanoparticles to the PVDF casting solution causes the α- to β-phase conversion [13,22]. As can be noted, the $F(\beta)$ values are similar within the studied CuONPs composition range (2-10 wt. %). This result could suggest that the crystallinity of the PVDF films is mainly influenced by the deposition onto the non-woven PET and not by the addition of CuONPs. Independently of the CuONPs not evidences of these were encountered in the ATR-FTIR spectrum. The absence of a peak corresponding to Cu-O strength at 532 cm^{-1} indicates that CuONPs are not present, at least, at the films surface.

In order to explore more deeply into the polymer films and detect the presence of CuONPs, Raman spectra to the PVDF films prepared at different concentrations of CuONPs were recorded. Raman spectra were recorded using a laser of 785 nm wavelength to guarantee its penetration into the sample. The Raman spectrum of the NWPET-PVDF (Figure 4), in the lower wavenumber region shows the characteristic signals of PVDF at 284, 410, 498 and 609 cm^{-1} [21]. The NWPET-PVDF films prepared with CuONPs, show three additional peaks at 297, 360 and 630 cm^{-1} (arrows in Figure 4). These peaks are assigned to the three Raman active modes of the CuO ($A_g + 2B_g$) evidencing the presence of the CuONPs embedded into the polymer matrix [23].

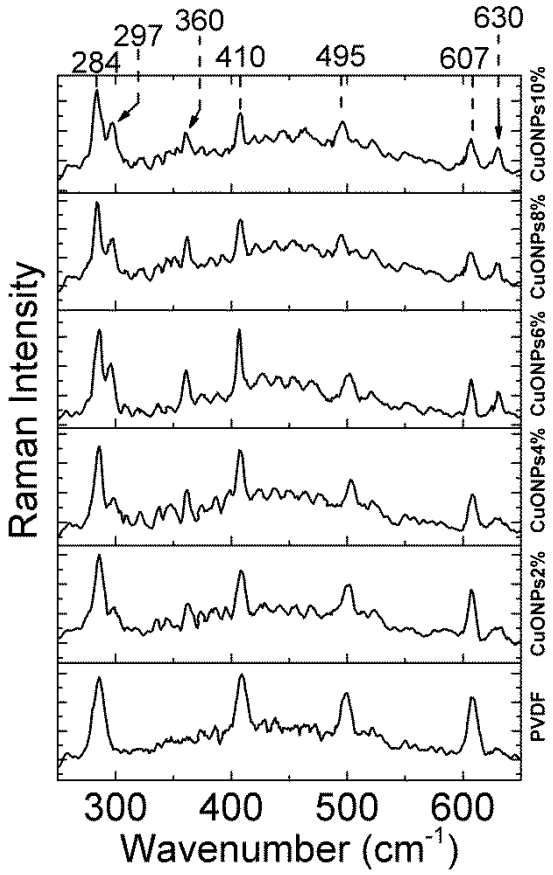

Figure 4. Raman spectra of the NWPET-PVDF membranes prepared at different CuONPs/PVDF wt.%.

A possible explanation of the absence of CuONPs on the NWPET-PVDF surface is due to their relatively easy dispersability in water, the precipitation kinetics of the polymer and the diffusion rate of the CuONPs through the polymer media. The rapid precipitation of the polymer, upon sinking the PVDF impregnate NWPET in water, causes that the CuONPs near to the interface escapes from it. Although, the diffusion of CuONPs in the inner of the PVDF is slow due to the high viscosity of

the media giving raise to the retention of nanoparticles during the precipitation process. It is likely that the CuONPs are present deeper in the pores of NWPET-PVDF membranes[14].

3.3 SEM characterization

To analyze the pore morphologies of the prepared membranes at different CuONPs compositions, the corresponding cross-section SEM micrographs were recorded (Figure 5). The membranes are composed from a top PVDF layer attached to a second one formed by the NWPET fabric (Figure 1). The PVDF and NWPET layers exhibit pores with finger-like and sponge-like morphologies, respectively. The size of PVDF and NWPET pores is in the order of micrometers and nanometers, respectively. This pattern was observed in all the prepared membranes (Figure 5).

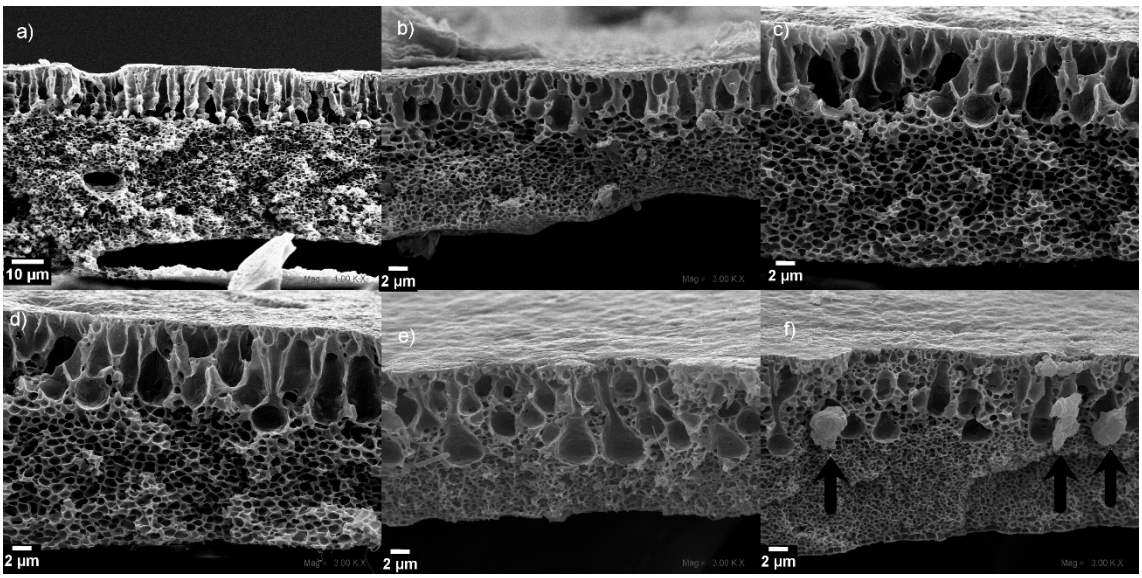

Figure 5. Cross-section SEM micrographs of the PVDF-NWPET samples a) neat PVDF-NWPET and b-f) doped with 2, 4, 6, 8, 10% of CuONPs; respectively. The scale bars represent 2 µm, unless a) (0 %) that is 10 µm.

The finger-like pores of the composite membranes in absence of CuONPs, appears aligned and extended to the center of the membrane in a compact distribution. The sponge-like and finger-like porous layers are well defined by a linear boundary along all the membrane as can be observed in Figure 5a.

The addition of the CuONPs to the casting solution causes the loss of the mentioned above linear boundary even at lower concentrations. Although, at 2 wt.% of CuONPs the linear finger-like structures dominates the morphology (Figure5b). By increasing the CuONPs content to 4 wt.% and 6 wt.%, Figure 5c and 5d; respectively, the pores adopt a tear-like morphology. Interestingly, at higher amounts of CuONPs (over 6 %), the sponge-like layer growth upward to the surface, surrounding and therefore diminishing the number of tear-like pores (Figure 5e). At the highest amount of CuONPs (10%), the membrane morphology is dominated by the sponge-like structure with certain micropores, apparently from the collapsing of the tear-like pores. Additionally, at this concentration some crystalline structures located at the boundary between the sponge and tear-like pores are observed (Figure 5f, arrows). These structures should correspond to the CuONPs due to at high concentration tends to aggregates to diminish the excess of surface energy related with their size. It is possible to infer that under the used conditions, this aggregation occurred at concentration higher than 8 wt.%, since in the other cross-sectioned SEM micrographs (wt.% < 8%) these structures were not observed. Similar results have been reported in mixed composite PVDF membranes prepared in presence of graphene oxide and Cu_xO (x=1 or 2) nanoparticles [14,15].

The presence of CuONPs not only affected the morphology of the finger-like layer but also the depth of these have a markedly decrease at the lowest CuONPs content (2%) (Figure 6). The addition of 2% of CuONPs causes an increase in the viscosity of the solution [14]. Consequently, the ability of water to penetrate into the casting solution and form finger-like pores decrease. As can be noted, with the 2% of CuONPs, this effect is clearly noted. The increasing in the CuONPs content not dramatically affected the pore depth (Figure 6, left panel. Additionally, the increasing of the CuONPs amount causes that both the pore size of the sponge-like structure and layer thickness decrease (Figure 6, right panel).

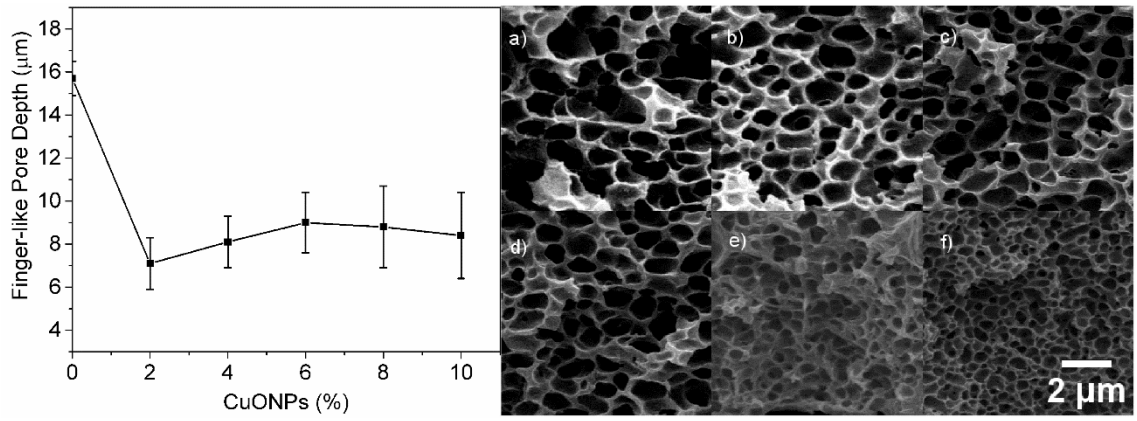

Figure 6. Effect of the CuONPs wt.% in the depth of the finger-like pores (left panel). SEM micrographs of the sponge-like layer at different CuONPs content; a) 0 wt.%, b) 2 wt.%, c) 4 wt.%, d) 6 wt.%, e) 8 wt.% and f) 10 wt.%). All images has the same size.

The distribution, morphology and size of the pores in the PVDF membranes are influenced by the contribution of the thermodynamic and the kinetic factors during the precipitation of the polymer (demixing process). Thermodynamically, the higher the instability of the casting solution, the high the demixing rate during the phase separation process. Therefore, more finger-like structures and less sponge-like structures are formed. From the kinetic perspective, the higher the viscosity of the casting solution, the lower the solvent/non-solvent exchange rate which causes a retard in the demixing process. This retard results in the formation of less finger-like structure and more sponge-like structure [24]. Therefore, we can suggest that the addition of CuONPs did not affects the stability of the polymer solution (thermodynamic) during the demixing process, but the precipitation rate (kinetic) due to the increase of the solution viscosity. Therefore, the membranes structures here obtained are dominated by kinetics and not by thermodynamics of the phase separation process.

3.4 Contact angle measurements

A crucial factor in the efficiency of the MD processes is the membrane hydrophobicity. In a membrane, this parameter depends on its roughness and surface energy [24] Therefore, the hydrophobicity of the obtained NWPET-PVDF composite membranes was evaluated by WAC measurements (Figure 7).

Peer-reviewed version available at Polymers 2018, 10, 862; doi:10.3390/polym10080862

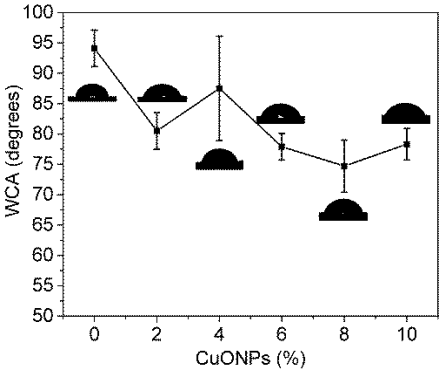

Figure 7. Dependence of the water contact angle with the amount of CuONPs (wt.%).

In absence of CuONPs, the NWPET-PVDF membrane shows a WCA higher than 90°, a characteristic value for hydrophobic materials. By preparing the membrane with 2 wt.% of CuONPs, the WCA decreases by c.a. 15 degrees, indicating a less hydrophobic character. Further increase in the CuONPs content, i.e from 4 wt.% to 10 wt.% lead to a slow decrease in the WCA.

As was mentioned before, by ATR-FTIR, CuONPs were not detected at the membrane surface. Additionally, the $F(\beta)$ values did not varied with the CuONPs wt.%. From these two results, we can suggest that the decrease in the hydrophobicity should not be related to a decrease in the surface energy but to changes in the roughness of the membranes upon the addition of nanoparticles.

Figure 8 shows the surface and top skin cross-section SEM micrograph taken to the NWPET-PVDF membranes prepared in absence (0 %) and presence of the CuONPs (2 to 10 wt.%). The neat NWPET-PVDF membrane (Figure 8a) shows a porous and rough surface with pores sizes larger than 200 nm. The addition of 2 wt.% of CuONPs to the casting solution causes that both, the surface roughness and the pore sizes on itdecrease (< 200 nm) (Figure 8b). The trend to decrease of both parameters continue by increasing the CuONPs wt.% from 4% to 10% (Figure 8c-f). At 10 wt.% of CuONPs, an smooth and quasi absent of pores surface was obtained.

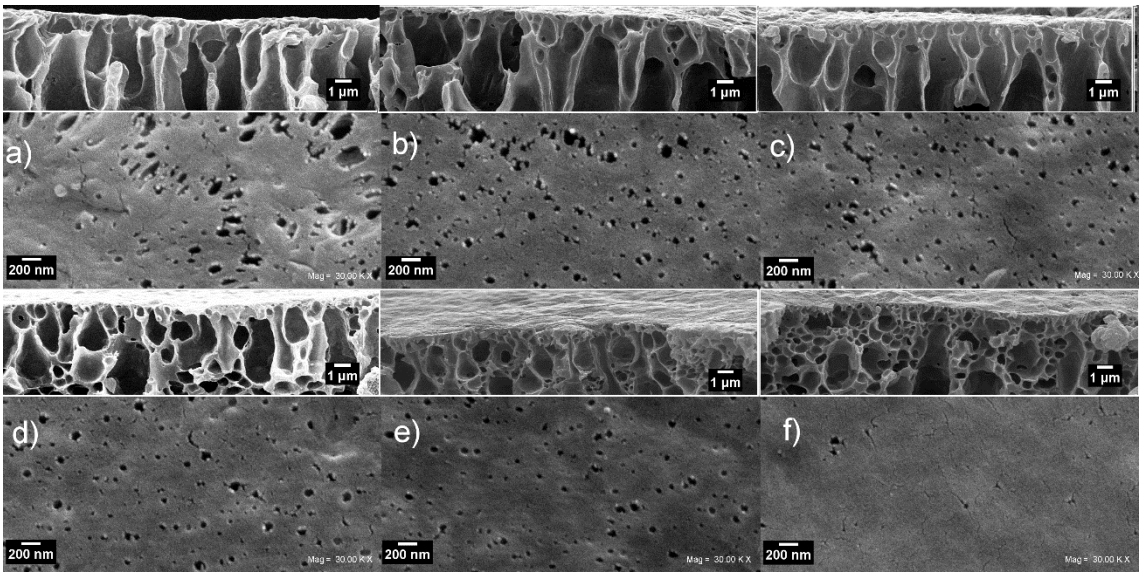

Figure 8. Top and cross-section SEM micrographs of the NWPET-PVDF membranes prepared a) in absence (wt. 0%) and b-f) presence of CuONPs (2, 4, 6, 8 and 10 wt.%; respectively). Scale bars of top-view= 200 nm, cross-section= 1 µm.

By a simple inspection of the rectangles inset on top of each figure, it is possible to note that the increases of the CuONPs wt.%, lead to a decrease of the micropores extended to the surface and an increase in the amount of nanopores just below the membrane surface. The change in the pore

distribution should be the responsible of the decrease of the surface roughness and hence the observed decrease in the WCA measurements upon the addition of CuONPs.

4. Conclusions

PVDF membranes with different wt.% of CuONPs embedded and supported in NWPET can be prepared by the phase inversion method. The deposition of PVDF solution on NWPET leads to an enhancement of the polar β-phase of the deposited polymer, which no varies with the amount of CuONPs. In these composites membranes the CuONPs are located in the inner of the membrane. The resulting membranes become less hydrophobic upon the addition of the nanoparticles. We suggest that the loss in its hydrophobicity arises from the decrease of the membrane roughness and not due to changes in its surface energy.

Acknowledgements:

The authors acknowledge to the project Corfo 13CEI2-21803 for the financial support.

References

1. Drioli, E.; Ali, A.; Macedonio, F. Membrane distillation: Recent developments and perspectives. *Desalination***2015**, *356*, 56–84, doi:10.1016/j.desal.2014.10.028.
2. Alkhudhiri, A.; Darwish, N.; Hilal, N. Membrane distillation: A comprehensive review. *Desalination***2012**, *287*, 2–18, doi:10.1016/j.desal.2011.08.027.
3. Hou, D.; Dai, G.; Wang, J.; Fan, H.; Zhang, L.; Luan, Z. Preparation and characterization of PVDF/nonwoven fabric flat-sheet composite membranes for desalination through direct contact membrane distillation. *Sep. Purif. Technol.***2012**, *101*, 1–10, doi:10.1016/j.seppur.2012.08.031.
4. Kang, G. dong; Cao, Y. ming Application and modification of poly(vinylidene fluoride) (PVDF) membranes - A review. *J. Memb. Sci.***2014**, *463*, 145–165, doi:10.1016/j.memsci.2014.03.055.
5. Khayet, M.; Mengual, J. I.; Matsuura, T. Porous hydrophobic/hydrophilic composite membranes: Application in desalination using direct contact membrane distillation. *J. Memb. Sci.***2005**, *252*, 101–113, doi:10.1016/j.memsci.2004.11.022.
6. Warsinger, D. M.; Swaminathan, J.; Guillen-Burrieza, E.; Arafat, H. A.; Lienhard V, J. H. Scaling and fouling in membrane distillation for desalination applications: A review. *Desalination***2015**, *356*, 294–313, doi:10.1016/j.desal.2014.06.031.
7. Tijing, L. D.; Woo, Y. C.; Choi, J.-S.; Lee, S.; Kim, S.-H.; Shon, H. K. Fouling and its control in membrane distillation—A review. *J. Memb. Sci.***2015**, *475*, 215–244, doi:10.1016/j.memsci.2014.09.042.
8. Qin, A.; Li, X.; Zhao, X.; Liu, D.; He, C. Engineering a highly hydrophilic PVDF membrane via binding TiO<inf>2</inf> nanoparticles and a PVA layer onto a membrane surface. *ACS Appl. Mater. Interfaces***2015**, *7*, 8427–8436, doi:10.1021/acsami.5b00978.
9. Wan, H.; Briot, N. J.; Saad, A.; Ormsbee, L.; Bhattacharyya, D. Pore functionalized PVDF membranes with in-situ synthesized metal nanoparticles: Material characterization, and toxic organic degradation. *J. Memb. Sci.***2017**, *530*, 147–157, doi:10.1016/j.memsci.2017.02.021.
10. Gao, J.; Huang, X.; Xue, H.; Tang, L.; Li, R. K. Y. Facile preparation of hybrid microspheres for super-hydrophobic coating and oil-water separation. *Chem. Eng. J.***2017**, *326*, 443–453, doi:10.1016/j.cej.2017.05.175.
11. Dong, C.; He, G.; Li, H.; Zhao, R.; Han, Y.; Deng, Y. Antifouling enhancement of poly(vinylidene fluoride) microfiltration membrane by adding Mg(OH)2nanoparticles. *J. Memb. Sci.***2012**, *387–388*, 40–47, doi:10.1016/j.memsci.2011.10.007.

12. Ng, L. Y.; Mohammad, A. W.; Leo, C. P.; Hilal, N. Polymeric membranes incorporated with metal/metal oxide nanoparticles: A comprehensive review. *Desalination***2013**, *308*, 15–33, doi:10.1016/j.desal.2010.11.033.

13. Dutta, B.; Kar, E.; Bose, N.; Mukherjee, S. Significant enhancement of the electroactive β-phase of PVDF by incorporating hydrothermally synthesized copper oxide nanoparticles. *RSC Adv.***2015**, *5*, 105422–105434, doi:10.1039/C5RA21903E.

14. Baghbanzadeh, M.; Rana, D.; Matsuura, T.; Lan, C. Q. Effects of hydrophilic CuO nanoparticles on properties and performance of PVDF VMD membranes. *Desalination***2015**, *369*, 75–84, doi:10.1016/j.desal.2015.04.032.

15. Zhao, C.; Lv, J.; Xu, X.; Zhang, G.; Yang, Y.; Yang, F. Highly antifouling and antibacterial performance of poly (vinylidene fluoride) ultrafiltration membranes blending with copper oxide and graphene oxide nanofillers for effective wastewater treatment. *J. Colloid Interface Sci.***2017**, *505*, 341–351, doi:10.1016/j.jcis.2017.05.074.

16. Qtaishat, M.; Rana, D.; Khayet, M.; Matsuura, T. Preparation and characterization of novel hydrophobic/hydrophilic polyetherimide composite membranes for desalination by direct contact membrane distillation. *J. Memb. Sci.***2009**, *327*, 264–273, doi:10.1016/j.memsci.2008.11.040.

17. Pastoriza-Santos, I.; Liz-Marzán, L. M. Formation and Stabilization of Silver Nanoparticles through Reduction by N,N-Dimethylformamide. *Langmuir***1999**, *15*, 948–951, doi:10.1021/la980984u.

18. Pastoriza-Santos, I.; Liz-Marzán, L. M. Formation of PVP-Protected Metal Nanoparticles in DMF. *Langmuir***2002**, *18*, 2888–2894, doi:10.1021/la015578g.

19. Schneider, C. A.; Rasband, W. S.; Eliceiri, K. W. NIH Image to ImageJ: 25 years of image analysis. *Nat. Methods***2012**, *9*, 671.

20. Sencadas, V.; Gregorio, R.; Lanceros-Méndez, S. α to β phase transformation and microestructural changes of PVDF films induced by uniaxial stretch. *J. Macromol. Sci. Part B Phys.***2009**, *48*, 514–525, doi:10.1080/00222340902837527.

21. Simoes, R. D.; Job, A. E.; Chinaglia, D. L.; Zucolotto, V.; Camargo-Filho, J. C.; Alves, N.; Giacometti, J. A.; Oliveira, O. N.; Constantino, C. J. L. Structural characterization of blends containing both PVDF and natural rubber latex. *J. Raman Spectrosc.***2005**, *36*, 1118–1124, doi:10.1002/jrs.1416.

22. Kar, E.; Bose, N.; Das, S.; Mukherjee, N.; Mukherjee, S. Enhancement of electroactive β phase crystallization and dielectric constant of PVDF by incorporating GeO_2 and SiO_2 nanoparticles. *Phys. Chem. Chem. Phys.***2015**, *17*, 22784–22798, doi:10.1039/C5CP03975D.

23. Xu, J. F.; Ji, W.; Shen, Z. X.; Li, W. S.; Tang, S. H.; Ye, X. R.; Jia, D. Z.; Xin, X. Q. Raman spectra of CuO nanocrystals. *J. Raman Spectrosc.***1999**, *30*, 413–415, doi:10.1002/(SICI)1097-4555(199905)30:5<413::AID-JRS387>3.0.CO;2-N.

24. Chen, Z.; Rana, D.; Matsuura, T.; Yang, Y.; Lan, C. Q. Study on the structure and vacuum membrane distillation performance of PVDF composite membranes: I. Influence of blending. *Sep. Purif. Technol.***2014**, *133*, 303–312, doi:10.1016/j.seppur.2014.07.015.